Suresh, L., Vaghasiya, J., Jones, M., & Tan, S. C. (2019). Biodegradable Protein-Based Photoelectrochemical Cells with Biopolymer Composite Electrodes That Enable Recovery of Valuable Metals. *ACS Sustainable Chemistry and Engineering*, *7*(9), 8834-8841. https://doi.org/10.1021/acssuschemeng.9b00790

Biodegradable protein-based photoelectrochemical cells with biopolymer composite electrodes that enable recovery of valuable metals

Lakshmi Suresh[1,†], Jayraj V. Vaghasiya[1,†], Michael R. Jones[2] and Swee Ching Tan[1*]

[1] Department of Materials Science and Engineering, National University of Singapore, 9 Engineering Drive 1, Singapore 117574

[2] School of Biochemistry, Biomedical Sciences Building, University of Bristol, University Walk, Bristol BS8 1TD, UK.

[†]Both authors have contributed equally to this manuscript.

*Corresponding author: msetansc@nus.edu.sg (S.C. Tan)

Abstract

The development of new technologies that use sunlight as an energy source is adding to pressure on finite natural resources and the challenges of recycling and disposal. Looking to nature for material assistance, we describe a proof-of-concept flexible and biodegradable photoelectrochemical cell based almost entirely on pigments, proteins, polysaccharides and graphene platelets. In addition to being largely environmentally benign, such devices present opportunities for the recovery of valuable components such as, in the present case, the geologically-scarce metal indium and the precious metal gold. Recovery is achieved through dissolution in ethanol followed by physical separation of the heavy element, leaving a residue made up from common elements that can be recycled through natural biodegradation. Potential applications for flexible, biomolecule-based photoelectrochemical cells are considered.

Keywords: Biodegradable, protein photoelectrochemical cell, flexible electrodes, indium recycling, graphene/ethyl-cellulose composite.

Introduction

Mankind is facing enormous challenges associated with the environmental impacts of synthetic waste materials that do not biodegrade. These have come into particular focus over the last few decades with the proliferation of electronic devices that not only require disposal after a relatively short lifetime but also utilize a range of elemental materials that are of limited availability.[1] Whilst new technological advances continue to address a range of global problems, including health, food security and energy supply, they also add to global concerns over the depletion of scarce natural resources and mankind's impact on the natural world. A case in point is the drive to address the challenges of future energy supply and the mitigation of climate change through the development and expansion of new technologies for solar energy conversion as alternatives to burning fossil fuels. Many major advances in this area have exploited naturally-occurring materials that are not abundant,[2] a good example being indium which is one of several elements that are key to modern electronics technology. It has been predicted that by 2020 some 91 % of globally-produced indium will be used in the form of indium tin oxide (ITO) for liquid crystal display (LCD) panels and other applications including photovoltaics,[3] and the demand for indium will outstrip supply by ~20 % (Supporting Fig. S1) due in the main to the expansion of photovoltaics and related technologies.[3,4] In accord with this it has recently been estimated that the total indium used in electronics industries in 2014 was more than double the production from mining.[5] Such findings raise questions over the long-term sustainability of new approaches to solar energy conversion and a wider range of electronic technologies.[2,4,5] Compounding the supply challenge, it has been estimated that only ~1 % of indium in flat panel displays is recovered at end-of-life,[4,6] the recycling and recovery of such a diffuse, high-value component being complicated by device architectures that involve robust materials such as glass and the presence of components that are potentially toxic.[5,7]

Interest in energy devices that are flexible, wearable, light-weight, inexpensive and produced from environmentally-friendly materials is longstanding.[8,9] In this work, we fabricated proof-of-concept flexible and biodegradable photoelectrochemical cells that employ bio-polymers as the electrode and photovoltaic components (Fig. 1a). Solar energy conversion was achieved using the RC-LH1 pigment-protein complex from the photosynthetic bacterium *Rhodobacter* (*Rba.*) *sphaeroides* as the photovoltaic component[10-14] and a water-soluble analogue of natural ubiquinone-10 (Coenzyme-Q_{10}) as a charge carrier (Fig. 1b). Both electrodes were based on ethyl-cellulose (EC - Fig. 1c), a derivative of the structural polysaccharide cellulose that is the most abundant biomolecule on the planet. Ethyl-cellulose is formed by treatment of cellulose to replace most of the three hydroxyl groups of each D-glucose moiety with ethyl ethers[15] (Fig. 1c). The result is a chemically inert, biocompatible and biodegradable polymer that is used in food and has potential as a coating for the

delivery of controlled-release drugs,[16] fertilizers,[17] herbicides[18] and pesticides.[19] In solar cell development, ethyl-cellulose has been used as a binder to attach conductive materials such as TiO_2 or graphene to a non-conducting glass substrate,[20,21,22] as an electrolyte gelling agent,[23] and a stabilizer for conducting graphene inks.[24] In the present context ethyl-cellulose has the advantage that it is hydrophobic, unlike cellulose, and can be dissolved in common solvents such as ethanol. It was cast as sheets that were optically-clear and flexible (Fig. 1d), enabling the assembly of deformable bio-photoelectrochemical cells, and was made conductive either by forming a composite with graphene nanoplatelets or by coating with ITO or Au. In addition to establishing the effectiveness and versatility of solar energy conversion in these flexible biopolymer-based cells compared to synthetic analogues, we demonstrate the ease of recovery of indium and gold from electrode materials and routes to cell disposal at end-of-life.

Experimental Section

Ethyl-cellulose and graphene nanoplatelets (6-8 nm thick, 15 μm diameter) were purchased from TCI Chemicals (Singapore). ITO and ITO-polyethylene terephthalate (PET) were purchased from Latech Scientific Supply (Singapore). Analytical reagent grade ethanol and ubiquinone-0 (Q_0 - 2-3-dimethoxy-5-methyl-*p*-benzoquinone, 98 %, Merck) were used as received. PufX-deficient RC-LH1 proteins from *Rba. sphaeroides* were purified as described previously[13,25] and stored as a concentrated solution in 20 mM Tris(tris(hydroxymethyl)aminomethane) (pH 8.0)/0.04% (w/v) n-dodecyl β-D-maltopyranoside at -80^{o}C before use.

To produce an electrode substrate, equal volumes (5 mL) of ethyl-cellulose and ethanol were mixed by stirring at room temperature for 12 hours to form a completely transparent amalgam. Electrodes were cast from this in 30 mm × 30 mm × 5 mm deep moulds on glass microscopy slides, using doctor blading to achieve a uniform electrode thickness. Cast electrode substrates were then annealed in air at 60 ºC for 20 minutes. To form the ITOEC electrode (resistance approximately 50 KΩ), a 300 nm thick layer of ITO was deposited onto the surface of a cast ethyl-cellulose substrate by RF sputtering.

To form GECC electrodes a mixture of ethyl-cellulose and graphene nanoplatelets was stirred at 500 rpm for 20 minutes at room temperature, sonicated for the same period, and then used to cast electrodes from an ethanolic solution as described above. The material was optimized by varying the ratio of ethyl-cellulose to graphene nanoplatelets and assessing its electrical conductivity. Cyclic voltammetry of 0.01 mM *N*,*N*,*N*′,*N*′-tetramethyl-p-phenylenediamine (TMPD) in Tris HCl (pH 7.4) was carried in a three-electrode configuration with GECC as the working electrode, a Pt-wire as the counter electrode and Ag/AgCl as the reference electrode, using an Autolab FRA32 potentiostat at a

scan rate of 20 mV s^{-1}.

Photoelectrochemical cells with an ITOEC/RC-LH1/Q_0/GECC architecture was fabricated by injecting 5 µL of a mixture of RC-LH1 protein and Q_0 electrolyte (concentrations 50 and 80 mM, respectively) into a cavity between a ITOEC front electrode and GECC back electrode of equal area that were separated using a 1 mm thick U-shaped piece of hot melt sealing foil. Cells were then immediately sealed using Araldite®. The ethyl-cellulose electrodes were left adhered to the glass slides for ease of handling during most electrical measurements. Cells with an ITOEC/RC-LH1/Q_0/AuEC architecture was constructed in the same way, the rear electrode comprising ethyl-cellulose sputtered with a 500 nm thick layer of Au. To form control cells with an ITO-PET/RC-LH1/Q_0/Au-PET architecture, ITO-PET was used as the front electrode and ITO-PET sputtered with 500 nm thick layer of Au was used as the back electrode. To form control cells with an ITO-glass/RC-LH1/Q_0/Au-glass architecture, commercial ITO-glass purchased from Latech Scientific Supply (Singapore) was used as the front electrode and this glass sputtered with a 500 nm thick layer of Au was used as the back electrode.

Photo-responses of cells were measured using a Keithley 2400 Source Meter under zero bias conditions with illumination from an incandescent lamp (100 mW cm^{-2}) to simulate sunlight (AM 1.5). The active area for all measurements was 0.20 cm^2. Strips of copper tape were used as current collectors for either electrode. After electrical measurements, several photo-electrochemical cells were buried 3 cm deep in natural soil (1 kg) obtained from West Coast Park in Singapore and used without any pre-treatment. Water was supplied at regular intervals to maintain the moisture of the soil. At 15-day intervals, cells were removed from the soil, washed with distilled water, dried, the electrode materials separated and weighed, and the average conductivity across the area of each electrode measured using a benchtop resistivity meter.

Cyclic bend-relax testing was done on ITOEC/RC-LH1/Q_0/GECC cells with an active area of 1.56 cm^2 on a lab-made apparatus. The edges of the cells were fixed and subjected to a bend angle of approximately 30◦. Photo-responses of the cells were measured using photo-chronoamperometry as described above, and the photocurrent density recorded once it had stabilised after each bend or relax event. Absolute photocurrents from ITOEC/RC-LH1/Q_0/GECC cells were lower in these measurements due to use of a lower intensity light source.

Results and Discussion

Ethyl-cellulose was fabricated into 9 cm^2 sections of electrode substrate by mixing thoroughly with ethanol, casting in a mould and annealing (see Methods), producing 3 mm thick optically-clear sheets (Fig. 2a). As ethyl-cellulose is not conducting, a graphene/ethyl-cellulose (GECC) composite

was also formed by mixing ethyl-cellulose with graphene nanoplatelets prior to dissolution in ethanol. A 60:40 (w:w) mix of ethyl-cellulose to nanoplatelets gave an optimal conductivity of 100 mS m^{-1} and resistance of ~1 KΩ. The morphology of the GECC electrode (Fig. 2b) was similar to that of plain ethyl-cellulose (not shown), confirming penetration of the conductive graphene nanoplatelets into the non-conductive ethyl-cellulose matrix. The catalytic response of this composite was tested by cyclic voltammetry using a well-characterized TMPD test electrolyte. The oxidation and reduction peak potentials of $TMPD^{\bullet+}/TMPD^{2+}$ were similar to those obtained with a Pt electrode (Fig. 2c), the lower maximum current response seen with GECC being expected for a composite of conductive and non-conductive materials. This comparable catalytic performance indicated the potential of GECC as a new, entirely biocompatible, electrode material.

X-ray diffraction (XRD) showed that plain ethyl-cellulose and the GECC were crystalline with unique diffraction peaks at 29.27^o and 26.19^o, respectively (Supporting Fig. S2). Crystallinity indices were 56.0 % and 92.8 %, respectively, indicating that the composite contained less amorphous material. A negligible shift (<1^o) in the diffraction peak angle for GECC in comparison to literature values for graphene oxide[26] indicated adequate relief of tensile stresses through proper curing, making the GECC comparable to commercial graphene oxide as an electrode material. In thermogravimetric analysis both electrode materials showed good stability up to 250 ^{o}C (Supporting Fig. S3).

To provide a counter electrode, cast sheets of ethyl-cellulose were sputtered with a 300 nm thick layer of ITO. This "ITOEC" electrode material showed substantially better average transmittance across the visible region than GECC and was also more highly transmitting in the near-IR where the RC-LH1 protein is most strongly absorbing (Fig. 2d), and so was selected as the front electrode. Averaged across the visible region its transmittance was ~22 % greater than for commercially-available ITO-coated glass. The transmittance of the ITOEC electrode material strongly declined at the high-energy end of the spectrum, indicating that the front electrode material could also shield the pigment-protein content of a photoelectrochemical cell from potentially damaging UV radiation.

Photoelectrochemical cells were fabricated by filling a cavity between ITOEC and GECC electrodes with a mixture of the RC-LH1 protein as the photovoltaic component and ubiquinone-0 (Q_0) as a water-soluble, mobile charge carrier (Fig. 1a). Under standard illumination these cells produced a short circuit current density (J_{SC}) of 16.3 μA/cm^2 and an open circuit voltage (V_{OC}) of 387 mV (Fig. 3a). An action spectrum of external quantum efficiency had a maximum value of 0.4 % at 860 nm (Fig. 3b), the line shape confirming the RC-LH1 protein as the source of the photo-response. In agreement, control cells lacking the photoprotein did not produce a photocurrent or photovoltage (data not shown). It is known that photoexcitation of the primary electron donor in the

RC-LH1 protein (P* - Fig 3c) initiates electron transfer to a bound ubiquinone (Q_B), producing the radical pair $P^+Q_B^-$ (Fig. 3c). Based on the direction of current flow and vacuum levels, we conclude that the role of Q_0 mediator was to transfer electrons from the quinone "terminal" of the RC-LH1 to the GECC back electrode, the circuit being completed by either direct or mediated reduction of the photo-oxidised "terminal" of the photoprotein by the ITOEC front electrode (Fig. 3c). The V_{OC} of 387 mV was comparable to the ~420 mV voltage gap between the mid-point potentials of the reaction centre P/P^+ couple and the Q_0/Q_0H_2 mediator.

The utility of ethyl-cellulose as an electrode substrate was compared with that of commercially-available flexible alternatives by constructing an RC-LH1/Q_0 cell with an ITOEC front electrode and a rear electrode comprising ethyl-cellulose sputtered with gold (AuEC). On illumination, a J_{SC} of 2.04 ± 0.1 μA/cm^2 and V_{OC} of 65 ± 1 mV was observed. The lower currents and voltages seen on replacing the GECC electrode with gold likely stems from the much larger potential gap between the Q_0/Q_0H_2 mediator and the electrode in the latter case. Promisingly, the performance of this cell was comparable to that of RC-LH1/Q_0 devices based on conventional electrode support materials PET and glass (see Methods). Under the same conditions, cells constructed from an ITO-coated PET front electrode and a Au-sputtered ITO-PET rear electrode produced a J_{SC} of 0.85 ± 0.05 μA/cm^2 and a V_{OC} of 73 ± 1 mV, (see Supporting Fig. S4) under the same conditions. Hence straight replacement of PET or glass by ethyl-cellulose did not have any negative impact on device performance. The effect of deformation of the EC electrode substrates on output was examined by subjecting an ITOEC/RC-LH1/Q_0/GECC cell to repeated bend-relax cycles under continuous illumination (see Methods). For each measurement the cell was bent, or unbent, and the current amplitude recorded once it had stabilised. The cell photocurrent increased on bending and dropped following relaxation, the average photocurrent density over 50 cycles being 9.2 μA/cm^2 while bent and 5.86 μA/cm^2 when relaxed (Fig. 3d). The photovoltage remained unchanged at ~0.3 V under either condition. This demonstrated that cells continued to operate when deformed and the reproducibility of the response under repeated application and release of stress indicated durability.

Recyclability of the ethyl-cellulose electrode materials was demonstrated by deconstructing cells used for photoelectrochemical measurements, burying the ITOEC and GECC electrodes in soil, and assaying them for weight and conductivity at 15-day intervals. Both electrode materials showed a >85 % loss of conductivity over 60 days, indicating a significant loss of structural integrity (Fig. 4a). The loss became greater over time for ITOEC, as might be expected given that the conductive layer was attached to the surface of the ethyl-cellulose rather than embedded as in the GECC. Both materials also showed a 12-18 % weight loss over this period (Fig. 4b), consistent with biodegradation of the ethyl-cellulose and release of ITO and graphene conductive materials into the surrounding soil.

We estimate that graphene and ITO each made up around 7 % of the total materials used to fabricate the cells (Supporting Fig. S5). As an additional evidence of this environmentally friendly concept, a set of 10 end of life devices were buried in a sunflower pot and monitored regularly over a period of 60 days (Supporting Fig. S6). There were no observable adverse effects on the health of the plant.

As outlined above, alongside questions over continuity of supply there is also concern that the growth of industries such as thin film solar photovoltaics will not be sustainable unless there is a dramatic change in the levels of end-of-life recovery of elements such as indium.[2] Addressing this, the use of a biopolymer as a degradable electrode material could also open the way to easier recovery of valuable components before disposal.

To demonstrate this, three 5 cm × 2 cm pieces of either ITOEC or AuEC electrode material were immersed overnight in 10 mL of absolute ethanol. Dense materials released from the ethyl-cellulose during that incubation were separated by centrifugation, washed with ethanol to remove any impurities, and pressed into discs of 1 cm diameter (Fig. 5a, b insets). X-ray diffraction (XRD) analysis of the pellet from ethanol treatment of the ITOEC material showed a predominant (112) peak at 26^{o}, identifying it as ITO,[27] whereas analysis of the pellet from ethanol treatment of the AuEC material showed a predominant (111) peak at 38.8^{o} identifying it as Au[28] (Fig. 5a, b). The percentage recovery of both ITO and Au was dependent on time and was complete (>98%) after around 12 hours dissolution in ethanol (Fig. 5c).

It is now well established that photosynthetic proteins can be used as solar energy converting materials in photoelectrochemical cells.[29-37] One often quoted advantage of using such proteins in light-powered or light-sensing devices is their inherently environmentally-benign character, being fabricated in living organisms from common elements and being subject to degradation and chemical recycling through natural processes. However, in order to realise a photoelectrochemical device these photosynthetic proteins have to be combined with synthetic electrolyte and electrode components that may either present physical or chemical problems to end-of-life disposal or contain elements that are relatively expensive or scarce. This detracts from the argument that pursuing research into the use of photosynthetic proteins in devices is worthwhile from the perspective of green technologies. In the case of purple bacterial photoproteins, the subject of this report, multiple laboratories have explored the fabrication of devices for solar energy conversion based on either a two or three electrode architecture. Popular choices for electrode materials in such devices include gold, silver, platinum, ITO-glass and FTO-glass.[29-37]A wide variety of mediators for charge transport have also been explored with Q_0, a water-soluble analogue of natural ubiquinone-10, being particularly effective.[38]

The purpose of the present study was to examine whether synthetic conducting substrates that are often employed as transparent electrode materials in such devices, particularly of a two-electrode

architecture, can be replaced by a biologically-derived alternative. We find that this was indeed the case, bio-photoelectrochemical cells employing ethyl-cellulose as a substrate for ITO and Au electrodes producing photocurrents and photovoltages that were similar to those from equivalent cells using ITO-PET as the substrate for the conductive coating. Ethyl-cellulose is more hydrophobic than natural cellulose, enabling the fabrication of photoelectrochemical cells with a liquid core, but is considered to be a benign, biodegradable material suitable as a coating for drug or chemical delivery. Ethyl cellulose spun fibres and cast sheets have been used in sensor and capacitor applications,[39-42] but not as an electrode substrate for a photoelectrochemical cell. In the present case it could be processed into a flexible, highly-transmitting electrode substrate through a simple process of casting and annealing at a moderate temperature.

To move away from the use of precious/scarce metals as coatings to render ethyl-cellulose conductive, an ethyl-cellulose composite was formulated using graphene nanoplatelets as the conducting material. Cells fabricated with an ITOEC/RC-LH1/Q_0/GECC architecture produced higher photocurrents and photovoltages than those with an ITOEC/RC-LH1/Q_0/AuEC architecture, demonstrating the utility of the composite as an electrode material for a bio-photoelectrochemical cell.

Although the ethyl-cellulose/graphene composite enabled fabrication of cells without a precious metal coating on the back electrode, these demonstration cells still included ITO to render the front electrode conductive. Experiments carried out on sections of electrode material showed that using ethyl-cellulose as a substrate enabled recovery of indium through a relatively simple process of ethanol solubilisation followed by physical separation, and the equivalent could be achieved using gold-coated ethyl-cellulose. In principle the suspension of ethyl-cellulose and ethanol remaining after metal separation could either be used to cast new sheets of electrode base or disposed of via a route such as composting or conversion to biofuels (give that the electrode material is sugar-based). Composting is also feasible for intact photoelectrochemical cells where both the photoprotein and quinone components are biodegradable. Soil burial tests demonstrated the first stages of such a process with loss of electrode conductivity and mass.

Another attribute of ethyl-cellulose as an electrode material is its ability to withstand substantive deformation by bending or twisting. Intact ITOEC/RC-LH1/Q_0/GECC cells still produced photocurrents on bending, the rise in steady current relative to the planar conformation likely being due to a decrease in electrode separation. In recent work we have demonstrated the used of the same photosynthetic RC-LH1 complex in a touch sensor “e-skin” based on flexible electrode materials, the basis of pressure sensing being dissipation of an inter-electrode voltage difference on decreasing the inter-electrode spacing.[43] It is conceivable that the ethyl-cellulose electrode materials

described here could replace the ITO-coated and gold-coated polyethylene terephthalate films used in that work, producing a biodegradable e-skin for transient applications.

Finally, the fabrication of a completely biodegradable and sustainable photoelectrochemical cell may be possible in future work. As an example, it may be possible to replace the ITO-coated EC front electrode with an electrode composed of cellulose nanofibers that are conductive due to a surface layer of carbon black nanoparticles, as described recently.[44] Combining this with the GECC composite as the back electrode would produce a cell in which both electrodes are formed from a combination of a sugar-based biopolymer and a conducting carbon nanomaterial.

Conclusions

In conclusion, this work demonstrates the fabrication of a photoelectrochemical cell in which photocurrents and photovoltages are generated by a natural photosynthetic protein enclosed between cellulose-based electrodes. As far as we are aware this is the first demonstration of the use of ethyl-cellulose as an electrode substrate, and the first description of use of an ethyl-cellulose/graphene composite in a photoelectrochemical cell. Cells based on ethyl-cellulose outperform otherwise equivalent cells based on PET, and their current and voltage outputs were maintained when deformed, opening doors to applications in flexible opto-electronics and sensing. Most components used in the demonstration cells are biocompatible and biodegradable, and components such ITO and Au used to render the cellulose-based electrodes conductive can be recovered through a simple chemical procedure utilising ethanol, producing components that can be easily recycled given their biological origins. The photocurrents and photovoltages produced by these demonstration bio-cells are modest in comparison to state-of-the-art silicon, dye sensitized, or polymer blend solar cells, but are already sufficient to enable varied sensing applications, some of which are also dependent on specific chemical interactions between the photoprotein and target molecules. The fabrication of novel electrode materials made from biology's most abundant organic polymer is likely to take research on photosynthetic biomaterials in interesting new directions in search of green solutions to the challenges of energy supply, climate change, environmental damage and the sustainability of technologies based on finite resources.

Associated content

Supporting information includes data on indium supply/demand, crystallinity, TGA, Photocurrent and photo voltage responses, cell composition and electrode disposal.

Acknowledgment

Lakshmi Suresh, Jayraj V. Vaghasiya, and Swee Ching Tan acknowledge the financial support from MOE AcRF 1 (R-284-000-161-114 and R-284-000-174-114). Michael R. Jones acknowledges support from the Biotechnology and Biological Sciences Research Council of the UK (project BB/I022570/1) and the BrisSynBio Synthetic Biology Research Centre (BB/L01386X/1).

Conflict of Interest

The authors declare no conflict of interest.

References

1. Widmer, R.; Oswald-Krapf, H.; Sinha-Khetriwal, D.; Schnellmann, M.; Boni, H., Global perspectives on e-waste. *Environ. Impact Assess. Rev.* **2005,** *25,* 436-458, DOI 10.1016/j.eiar.2005.04.001.
2. Fthenakis, V. Sustainability of photovoltaics: The case for thin-film solar cells. *Renew. Sustainable Energy Rev.* **2009,** *13,* 2746-2750, DOI 10.1016/j.rser.2009.05.001.
3. European Commission *Critical raw materials for the EU. Report of the Ad-hoc Working Group on defining critical raw materials: Annex V,* **2010**.
4. Moss, R. L.; Tzimas, E.; Kara, H.; Willis, P.; Kooroshy, J. *Critical metals in strategic energy technologies: assessing rare metals as supply-chain bottlenecks in low-carbon energy technologies; Publications Office of the European Union* (2011).
5. Zhang, S.; Ding, Y.; Liu, B.; Chang C. Supply and demand of some critical metals and present status of their recycling in WEEE. *Waste Management* **2017,** *65,* 113-127, DOI 10.1016/j.wasman.2017.04.003.
6. Lokanc, M.; Eggert, R.; Redlinger, M. *The Availability of Indium: The Present, Medium Term, and Long Term. National Renewable Energy Laboratory Report, U.S. Department of Energy*, **2015**.
7. Zhang, K.; Wu, Y.; Wang, W.; Li, B.; Zhang, Y.; Zuo, T. Recycling indium from waste LCDs: A review. *Resour. Conserv. Recycling* **2015**, *104,* 276-290, DOI 10.1016/j.wasman.2017.03.031.
8. H. Nishide, K. Oyaizu, Toward Flexible Batteries, *Science* **2008,** *319,* 737-738, DOI 10.1126/science.1151831.
9. Krebs, F. C., Biancardo, M., Winther-Jensen, B., Spanggard, H. and Alstrup, J. Strategies for incorporation of polymer photovoltaics into garments and textiles. *Sol. Energy Mater. Sol. Cells* **2006**, *90,* 1058–1067, DOI 10.1016/j.solmat.2005.06.003.
10. Siebert, C.A.; Qian, P.; Fotiadis, D.; Engel, A.; Hunter, C.N.; Bullough, P.A. Molecular architecture of photosynthetic membranes in *Rhodobacter sphaeroides*: the role of PufX. *EMBO*

J. **2004**, *23*, 690-700, DOI 10.1038/sj.emboj.7600092.

11. Qian, P.; Papiz, M.Z.; Jackson, P.J.; Brindley, A.A.; Ng, I.W.; Olsen, J.D.; Dickman, M.J.; Bullough, P.A.; Hunter, C.N. Three-dimensional structure of the *Rhodobacter sphaeroides* RC-LH1-PufX complex: dimerization and quinone channels promoted by PufX. *Biochemistry* **2013**, *52*, 7575-7585, DOI 10.1021/bi4011946.
12. Niwa, S.; Yu, L.-J.; Takeda, K.; Hirano, Y.; Kawakami, T.; Wang-Otomo, Z.-Y.; Miki, K. Structure of the LH1-RC complex from *Thermochromatium tepidum* at 3.0 Å. *Nature* **2014**, *508*, 228-232, DOI 10.1038/nature13197.
13. Ravi, S. K.; Yu, Z.; Swainsbury, D. J. K.; Ouyang, J.; Jones, M. R.; Tan, S. C. Tandem solar cells: enhanced output from biohybrid photoelectrochemical transparent tandem cells integrating photosynthetic proteins genetically modified for expanded solar energy harvesting. *Adv. Energy Mater.* **2017,** *7*, 1601821, DOI 10.1002/aenm.201770038.
14. Ravi, S. K.; Swainsbury D. J. K.; Singh, V. K.; Ngeow Y. K.; Jones, M. R.; Tan, S.C. A mechanoresponsive phase-changing electrolyte enables fabrication of high-output solid-state photobioelectrochemical devices from pigment-protein multilayers. *Adv. Mater.* **2018,** *30*, 1704073, DOI 10.1002/adma.201704073.
15. Koch W. Properties and uses of ethylcellulose. *Ind. Eng. Chem.* **1937,** *29*, 687-690, DOI 10.1021/ie50330a020.
16. Siepmann, F.; Siepmann, J.; Walther, M.; MacRae, R. J.; Bodmeier, R. Polymer blends for controlled release coatings. *J. Control. Release* **2008,** *125*, 1-15, DOI 10.1016/j.jconrel.2007.09.012.
17. Pérez-García, S.; Fernández-Perez, M.; Villafranca-Sanchez, M.; González-Pradas, E.; Flores-Céspedes, F. Controlled release of ammonium nitrate from ethylcellulose coated formulations. *Ind. Eng. Chem. Res.* **2007,** *46*, 3304-3311, DOI 10.1021/ie061530s.
18. Sopena, F.; Cabrera, A.; Maqueda, C.; Morillo, E. Controlled release of the herbicide norflurazon into water from ethylcellulose formulations. *J. Agric. Food Chem.* **2005,** *53*, 3540-3547, DOI 10.1021/jf048007d.
19. Roy, A.; Singh, S. K.; Bajpai, J.; Bajpai, A. K. Controlled pesticide release from biodegradable polymers. *Cent. Eur. J. Chem.* **2014,** *12*, 453-469, DOI 10.2478/s11532-013-0405-2.
20. Zhang, D. W.; Li, X. D.; Li, H. B.; Chen, S.; Sun, Z.; Yin, X. Z.; Huang, S. M. Graphene-based counter electrode for dye-sensitized solar cells. *Carbon* **2011**, *49*, 5382-5388, DOI 10.1016/j.carbon.2011.08.005.
21. Liu, T.-C.; Wu, C. C.; Huang, C. H.; Chen C. M. Effects of ethyl cellulose on performance of titania photoanode for dye-sensitized solar cells. *J. Electron. Mater.* **2016,** *45*, 6192-6199, DOI

10.1007/s11664-016-4719-7.

22. Im, D.; H. Hyun, S.; Y. Park, S.; Y. Lee, B.; Kim, Y. H., Preparation of high dispersed nickel pastes for thick film electrodes. *J. Mater. Sci*. **2006**, *41*, 6425-6430, DOI 10.1007/s10853-006-0715-2.
23. Neo, C. Y.; Ouyang J. Ethyl cellulose and functionalized carbon nanotubes as a co-gelator for high-performance quasi-solid state dye-sensitized solar cells. *J. Mater. Chem. A* **2013,** *1*, 14392-14401, DOI 10.1039/C3TA13217J.
24. Secor, E. B., Prabhumirashi, P. L., Puntambekar, K., Geier, M. L. and Hersam, M. C. Inkjet printing of high conductivity, flexible graphene patterns. *J. Phys. Chem. Lett.* **2013**, *4*, 1347-1351, DOI 10.1021/jz400644c.
25. Friebe, V. M.; Delgado, J. D.; Swainsbury, D. J. K.; Gruber, J. M.; Chanaewa, A.; van Grondelle, R.; von Hauff, E.; Millo, D.; Jones, M. R.; Frese. R. N. Plasmon-enhanced photocurrent of photosynthetic pigment proteins on nanoporous silver. *Adv. Funct. Mater.* **2016,** *26*, 285-292, DOI 10.1002/adfm.201504020.
26. Liu, G.; Wang, L.; Wang, B.; Gao, T.; Wang, D. A reduced graphene oxide modified metallic cobalt composite with superior electrochemical performance for supercapacitors. *RSC Adv.***2015,** *5*, 63553-63560, DOI 10.1039/C5RA09748G.
27. Simchi, H.; McCandless, B.; Meng, T.; Shafarman, W. Structure and interface chemistry of MoO3 back contacts in Cu(In,Ga)Se2 thin film solar cells. *J. Appl. Phys.* **2014,** *115*, 033514, DOI 10.1063/1.4862404.
28. Farooq, M. U.; Novosad, V.; Rozhkova, E. A.; Wali, H.; Ali, A.; Fateh, A. A.; Neogi, P. B.; Neogi, A.; Wang, Z. Gold nanoparticles-enabled efficient dual delivery of anticancer therapeutics to HeLa cells. *Sci. Rep.* **2018,** *8*, 2907, DOI 10.1038/s41598-018-21331-y.
29. Badura A.; Kothe T.; Schuhmann W.; Rögner M. Wiring photosynthetic enzymes to electrodes. *Energy Environ. Sci.* **2011**, *4*, 3263-3274, DOI 10.1039/C1EE01285A.
30. Boghossian A. A.; Ham M.-H.; Choi J. H.; Strano M. S. Biomimetic strategies for solar energy conversion: a technical perspective. *Energy Environ. Sci.* **2011**, *4*, 3834-3843, DOI 10.1039/C1EE01363G.
31. Wang F.; Liu X.; Willner I. Integration of photoswitchable proteins, photosynthetic reaction centers and semiconductor/biomolecule hybrids with electrode supports for optobioelectronic applications. *Adv. Mater.* **2013**, *25*, 349-377, DOI 10.1002/adma.201201772
32. Kim Y.; Shin S. A.; Lee J.; Yang K. D.; Nam K. T. Hybrid system of semiconductor and photosynthetic protein. *Nanotechnology* **2014**, *25*, 342001, DOI 10.1088/0957-4484/25/34/342001.

33. Nguyen, K.; Bruce, B. D. Growing green electricity: Progress and strategies for use of Photosystem I for sustainable photovoltaic energy conversion. *Biochim. Biophys. Acta - Bioenerg.* **2014**, *1837*, 1553-1566, DOI 10.1016/j.bbabio.2013.12.013.
34. Yehezkeli, O.; Tel-Vered, R.; Michaeli, D.; Willner, I.; Nechushtai R. Photosynthetic reaction center-functionalized electrodes for photo-bioelectrochemical cells. *Photosynth. Res.* **2014**, *120*, 71-85, DOI 10.1007/s11120-013-9796-3.
35. Ravi, S. K.; Tan, S. C. Progress and perspectives in exploiting photosynthetic biomolecules for solar energy harnessing. *Energy Environ. Sci.* **2015**, 8, 2551-2573, DOI 10.1039/C5EE01361E.
36. Friebe, V. M.; Frese, R. N. Photosynthetic reaction center-based biophotovoltaics. *Curr. Opin. Electrochem.* **2017,** *5*, 126-134, DOI 10.1016/j.coelec.2017.08.001.
37. Ravi, S. K.; Udayagiri, V. S.; Suresh, L.; Tan, S. C. Emerging role of the band-structure approach in biohybrid photovoltaics: A path beyond bioelectrochemistry. *Adv. Funct. Mater.* **2017**, 28, 1, DOI 10.1002/adfm.201705305.
38. Friebe, V. M.; Swainsbury, D. J. K.; Fyfe, P. K.; van der Heijden, W.; Jones, M. R.; Frese, R. N. On the mechanism of ubiquinone mediated photocurrent generation by a reaction center based photocathode. *Biochim. Biophys. Acta* **2016**, *1857*, 1925-1934, DOI 10.1016/j.bbabio.
39. Kacmaz, S.; Ertekin, K.; Suslu, A.; Ozdemir, M.; Ergun, Y.; Celik, E.; Cocen, U. Emission based sub-nanomolar silver sensing with electrospun nanofibers. *Sens. Actuators B* **2011**, 153, 205-213, DOI 10.1016/j.snb.2010.10.036.
40. Oter, O.; Ertekin, K.; Kirilmis, C.; Koca M. Spectral characterization of a newly synthesized fluorescent semicarbazone derivative and its usage as a selective fiber optic sensor for copper(II). *Anal. Chim. Acta* **2007**, *584*, 308-314, DOI 10.1016/j.aca.2006.11.052.
41. Zhang, Q.; An, C.; Fan, S.; Shi, S.; Zhang, R.; Zhang, J.; Li, Q.; Zhang D.; Hu X.; Liu J. Flexible gas sensor based on graphene/ethyl cellulose nanocomposite with ultra-low strain response for volatile organic compounds rapid detection. *Nanotechnology* **2018**, *29*, 285501, DOI 10.1088/1361-6528/aabf2f.
42. Xiong, J.; Li, S.; Ye, Y.; Wang, J.; Qian, K.; Cui, P.; Gao, D.; Lin, M.-F.; Chen, T.; Lee, P. S., A deformable and highly robust ethyl cellulose transparent conductor with a scalable silver nanowires bundle micromesh. *Adv. Mater*. **2018**, *30*, 1802803, DOI org/10.1002/adma.201802803.
43. Ravi, S.K.; Wu, T.; Udayagiri, V.S.; Vu, X.M.; Wang, Y.; Jones, M.R.; Tan, S.C. Photosynthetic bioelectronic sensors for touch perception, UV-detection and nanopower generation: toward self-powered e-skins. *Adv. Mater.* **2018**, *30*, 1802290, DOI 10.1002/adma.201802290.
44. Kuang, Y.; Chen, C.; Pastel, G.; Li, Y.; Song, J.; Mi, R.; Kong, W.; Liu, B.; Jiang, Y.; Yang, K.;

Hu, L. Conductive cellulose nanofiber enabled thick electrode for compact and flexible energy storage devices. *Adv. Energy Mater.* **2018**, *8*, 1802398, DOI 10.1002/aenm.201802398.

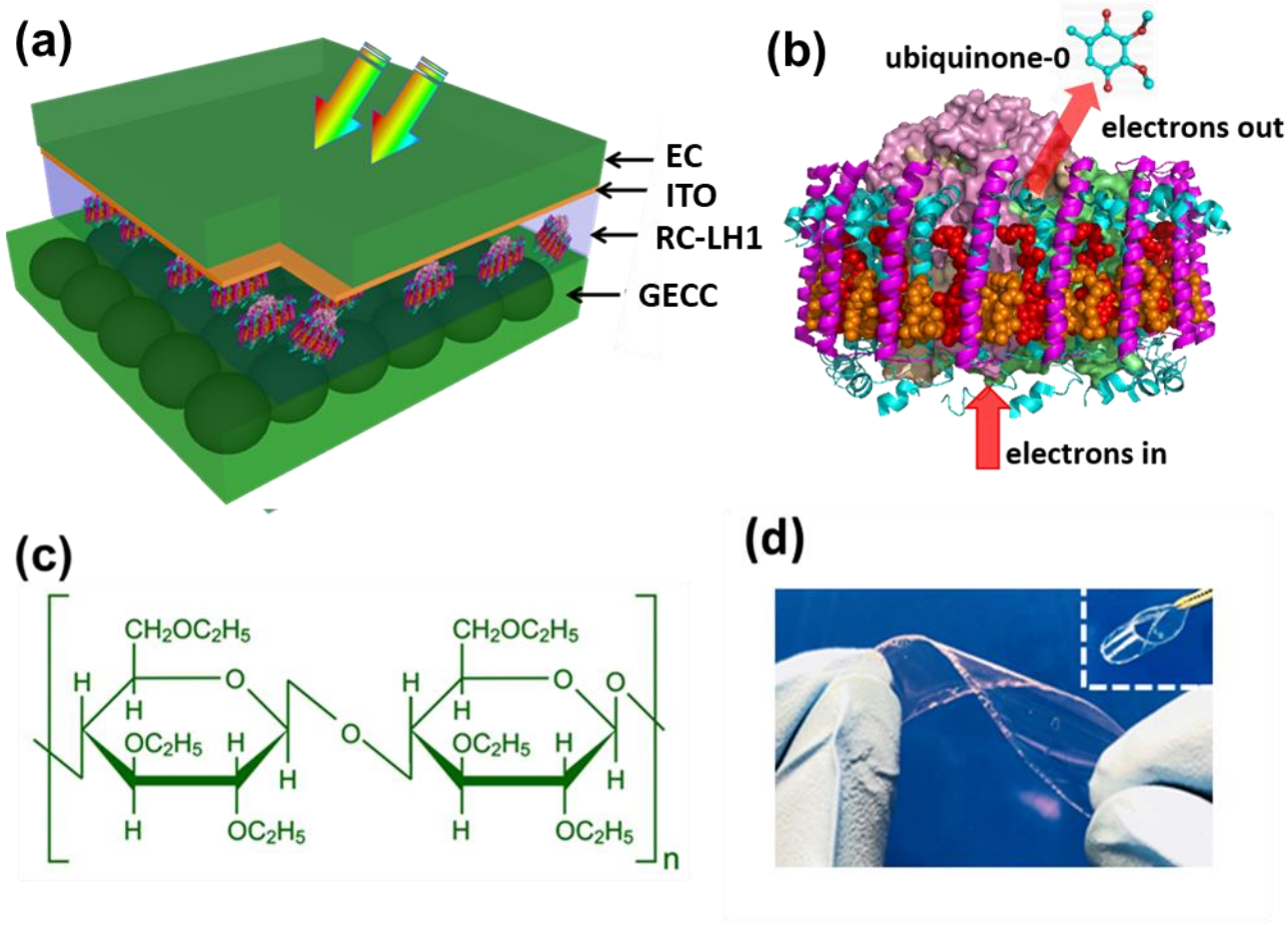

Figure 1. Cell architecture and composition. (a) Cells had a sandwich architecture with a blend of RC-LH1 protein and Q_0 mediator filling a cavity between an ITOEC front electrode and a GECC back electrode. Copper tape was used as a current collector. (b) The RC-LH1 complex from *Rba. sphaeroides* carries out photochemical charge separation with water-soluble Q_0 acting as an electron acceptor and charge carrier. (c) Molecular structure of the repeating unit of ethyl-cellulose, which comprises long, unbranched chains of β1→4 linked D-glucose moieties ethylated at their free -OH groups. (d) Cast and annealed ethyl-cellulose provides a flexible electrode substrate capable of undergoing repeated, reversible deformation.

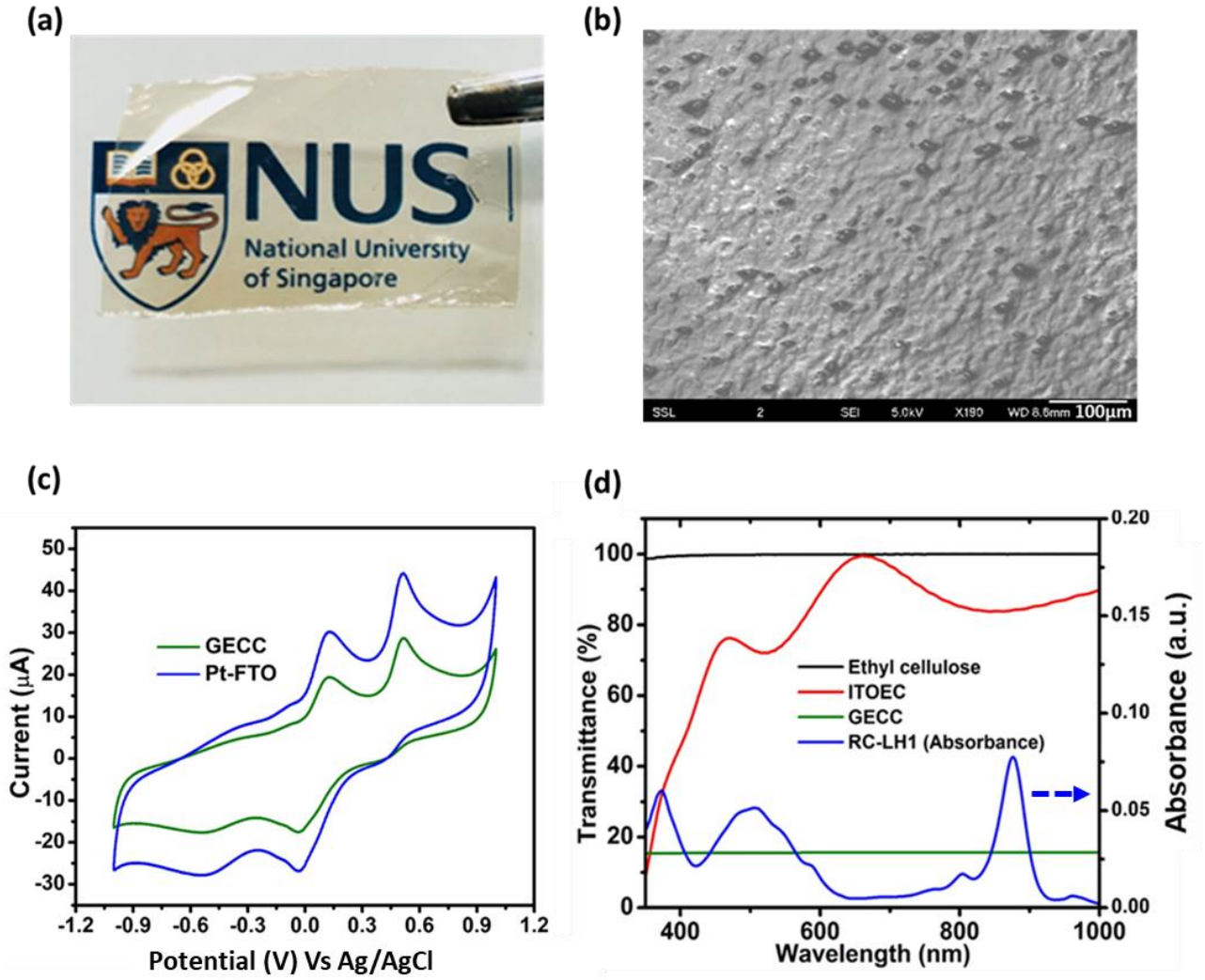

Figure 2. Properties of cell components. (a) Cast and annealed ITO-EC shows high transmittance across the visible region. (b) Scanning electron microscopy image of a GECC electrode. (c) Comparison of the catalytic activity of GECC and Pt electrodes against TMPD as a test electrolyte. (d) Transmittance of ethyl-cellulose remains high across most of the visible and near-IR when coated with ITO (selected as front electrode) but is uniformly lowered by embedded graphene nanoplatelets (selected as back electrode).

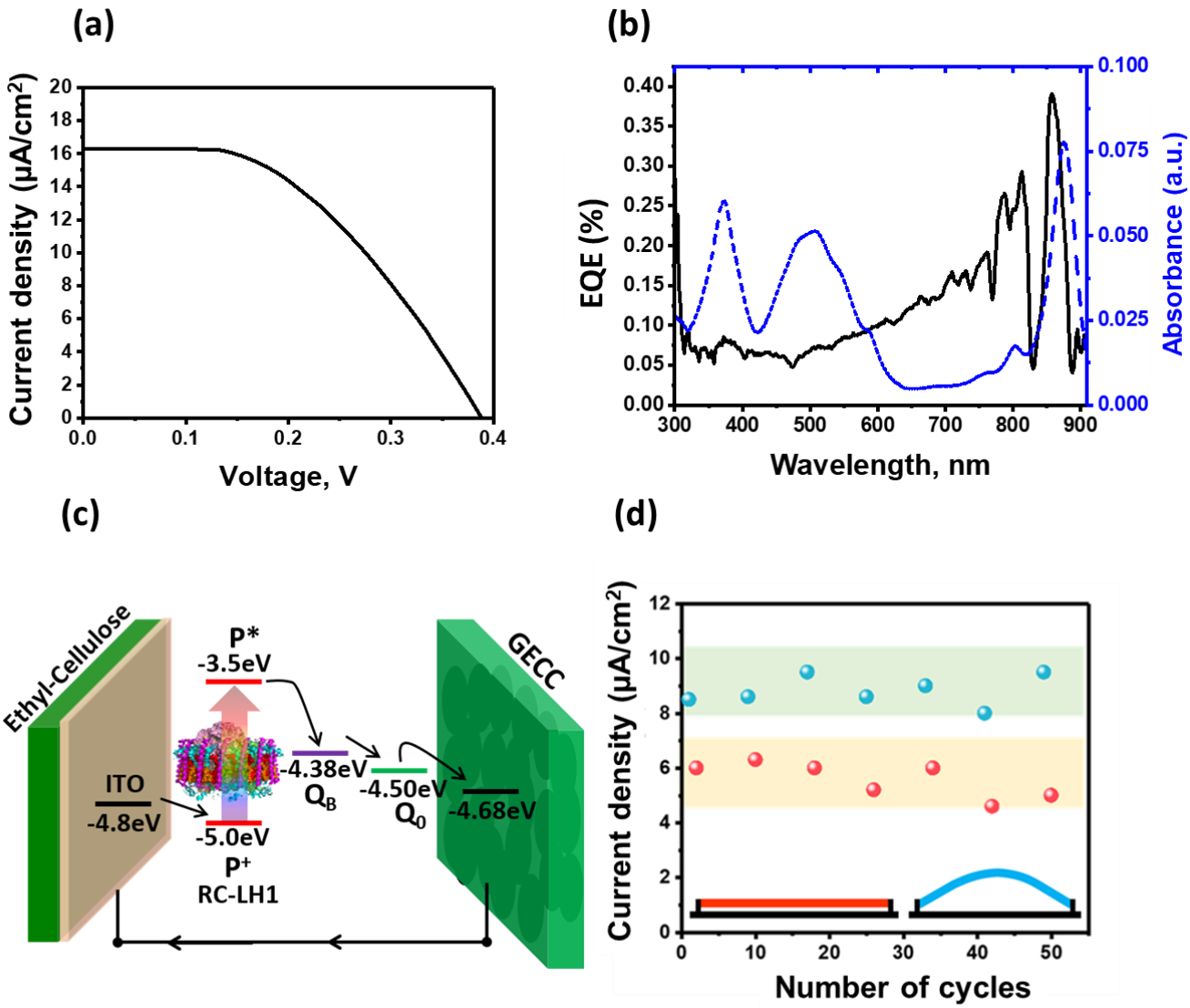

Figure 3. Output of an ITOEC/RC-LH1/Q_0/GECC cell and effects of deformation. (a) Photocurrent-voltage response under 100 mW/cm^2 illumination. (b) Action spectrum of external quantum efficiency compared to the absorbance spectrum of the RC-LH1 pigment-protein. (c) Schematic of cell mechanism; in cells where the GECC electrode was replaced by AuEC the energy level was changed to -5.1 eV. d) Stable photocurrent output under continuous white light illumination under bent (blue) or relaxed (red) conformations for 50 bend/relax cycles; data ranges are shaded and data points for every 8 cycles are shown. The photocurrent density was recorded after it had stabilised following each bend or relax event.

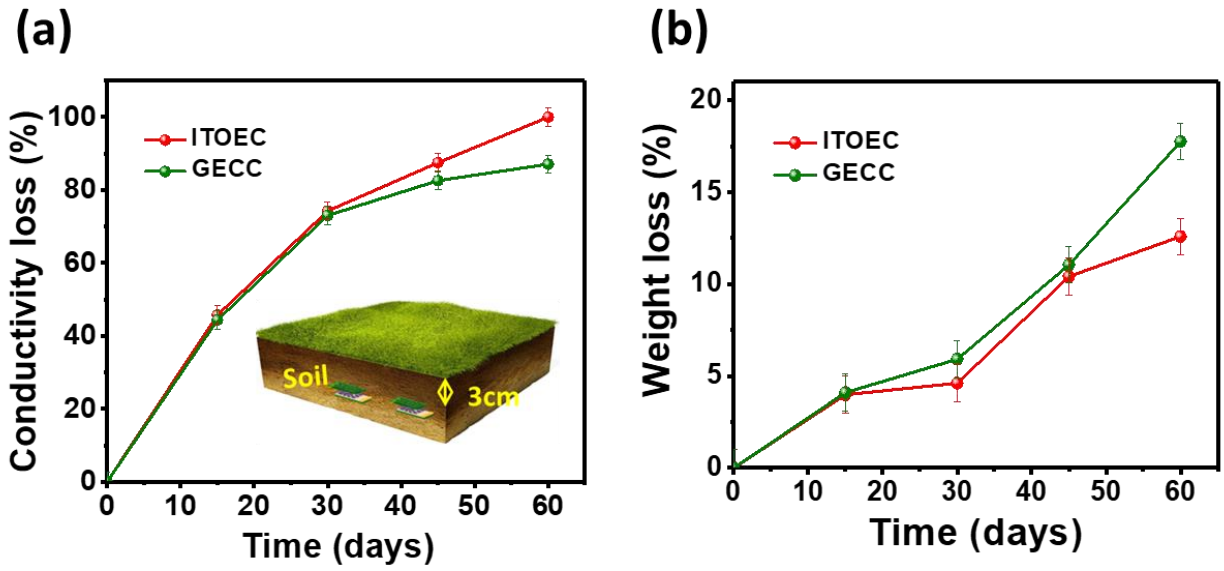

Figure 4. Biodegradation of discarded cells(a) Loss of electrode conductivity over 60 days of burial in soil. (b) Percentage loss of electrode weight over the same period.

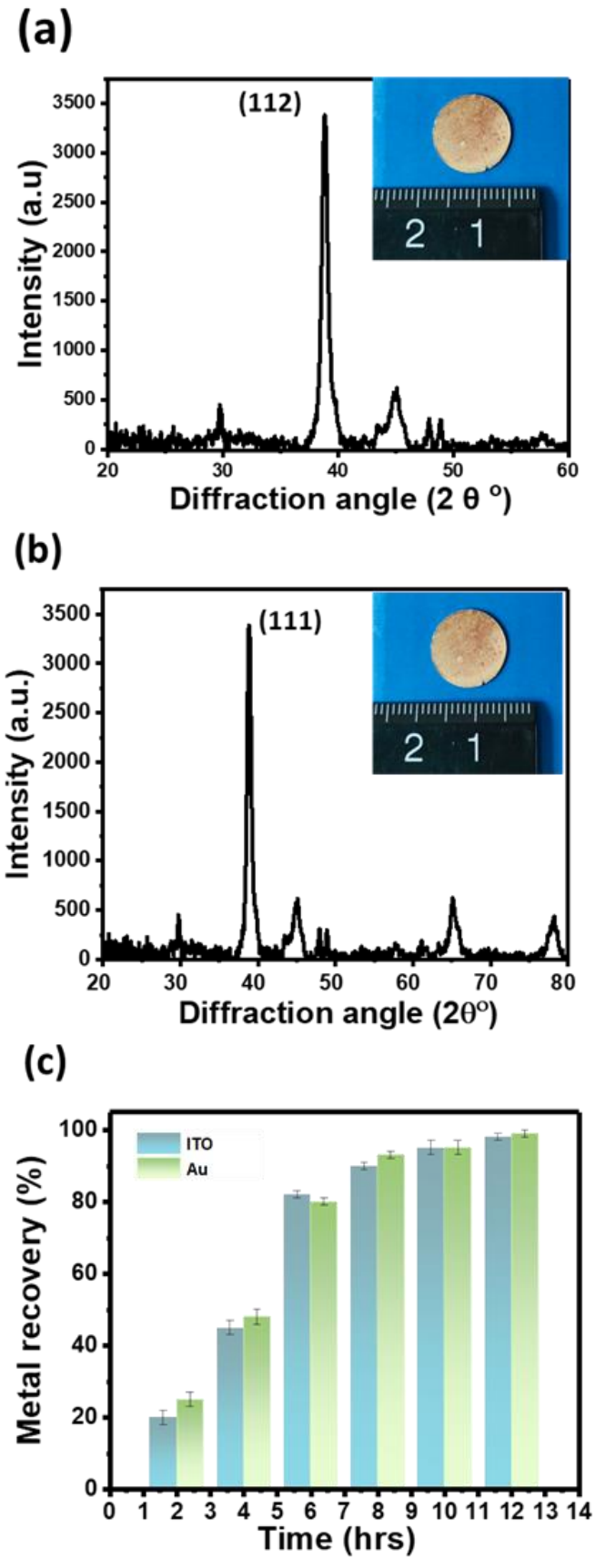
(a)
(112)
Intensity (a.u)
Diffraction angle (2 θ °)
(b)
(111)
Intensity (a.u.)
Diffraction angle (2θ°)
(c)
ITO
Au
Metal recovery (%)
Time (hrs)

Figure 5. Recovery of metals from electrode materials. (a) Loss of electrode conductivity over 60 days of burial in soil. b, Percentage loss of electrode weight over the same period. (c) Time dependence of metal recovery.

For Table of Contents Use Only

Graphical Abstract

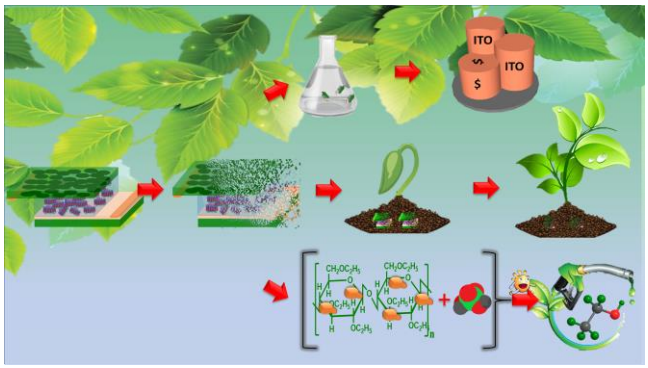

Novel biodegradable electrodes for bio photoelectrochemical cells with an ability to recover valuable components.

Supporting Information

Biodegradable protein-based photoelectrochemical cells with biopolymer-composite electrodes that enable recovery of valuable metals

Lakshmi Suresh[1,†], Jayraj V. Vaghasiya[1,†], Michael R. Jones[2] and Swee Ching Tan[1*]

[1] Department of Materials Science and Engineering, National University of Singapore, 9 Engineering Drive 1, Singapore 117574

[2] School of Biochemistry, Biomedical Sciences Building, University of Bristol, University Walk, Bristol BS8 1TD, UK.

[†]Both authors have contributed equally to this manuscript.

*Corresponding author: msetansc@nus.edu.sg (S.C. Tan)

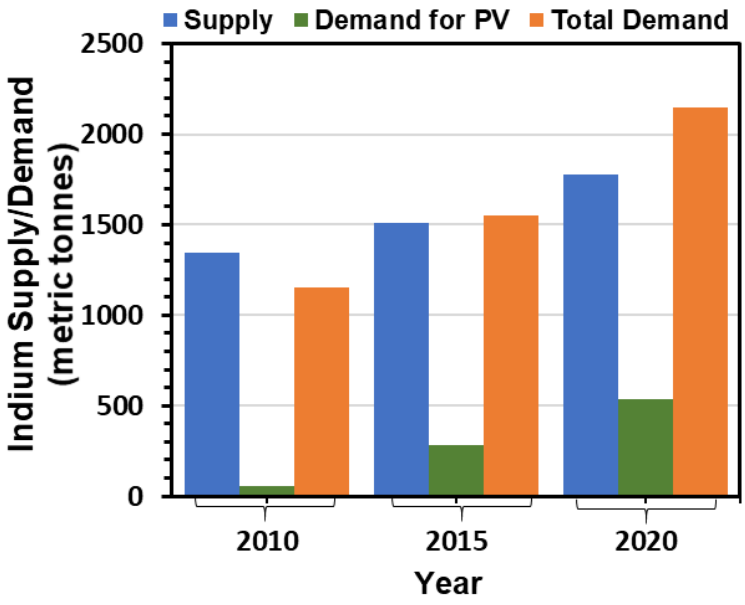

Supporting Figure S1. Predicted supply and demand of indium: Past and projected supply of primary indium (principally from zinc ores) and secondary indium (recycled from scraps) compared to demand for photovoltaics (PV) and total demand [S1].

S1. Moss, R. L.; Tzimas, E.; Kara, H.; Willis, P.; Kooroshy, J. *Critical metals in strategic energy technologies: assessing rare metals as supply-chain bottlenecks in low-carbon energy technologies; Publications Office of the European Union* (2011).

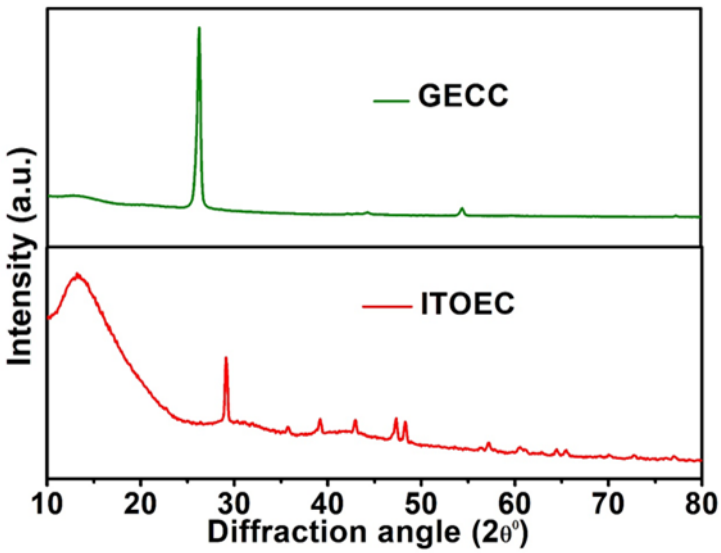

Supporting Figure S2. Crystallinity of electrode materials: X-ray diffraction spectra for the two electrode materials. X-ray diffraction was carried out using a copper kα target. The crystallinity index, a measure of the percentage of a material that is crystalline, was determined for each of the cellulose substrates by the peak height method (ratio of the height of the maximum peak I(002) and the I(AM) minimum) as described by Park *et al.* (2010).[S2] The crystallinity indices of the ethyl-cellulose substrate and GECC electrode material were 56.0 % and 92.8 % respectively, indicating that the composite contained less amorphous material.

S2. Park, S.; Baker, J.; Himmel, M.; Parilla, P.; Johnson, D. Cellulose crystallinity index: measurement techniques and their impact on interpreting cellulase performance. *Biotechnol. Biofuel.* **2010,** *3,* 10.

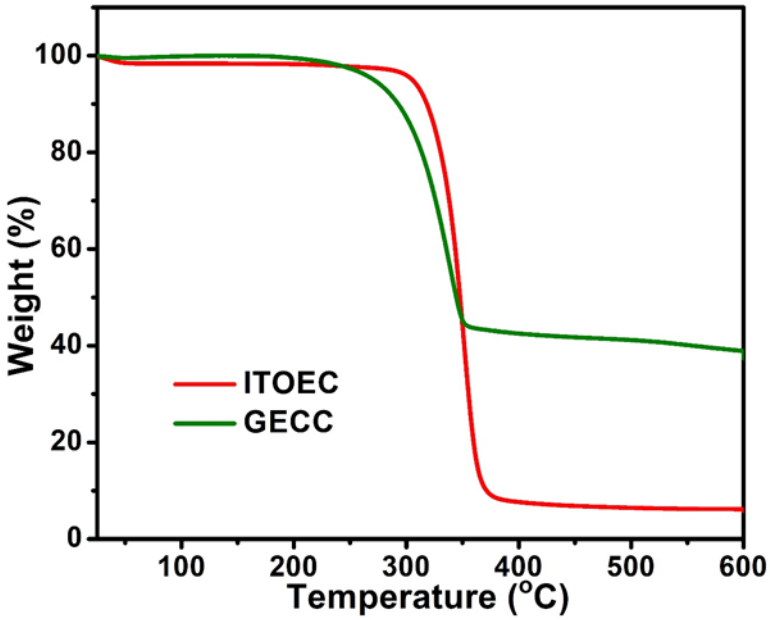

Supporting Figure S3. Thermogravimetric analysis of electrode materials: Thermogravimetric analysis was carried out at a heating rate of 10 ºC min^{-1} under a nitrogen atmosphere in a Q500 Thermogravimetric Analyzer (TA Instruments).

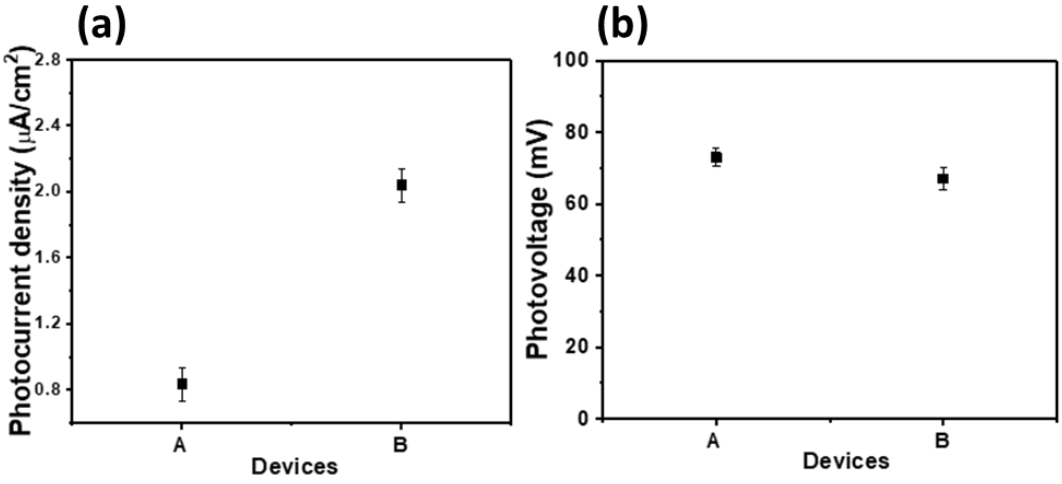

Supporting Figure S4. Cell output of electrode material: a-b, Photocurrent and photo voltage responses respectively of the two devices namely, A- ITO-PET/RC-LH1, Q_0/Au-ITO-PET (commercial electrodes) and B- ITOEC/RC-LH1, Q_0/AuEC (our substrate) under light illumination for 30s**.**

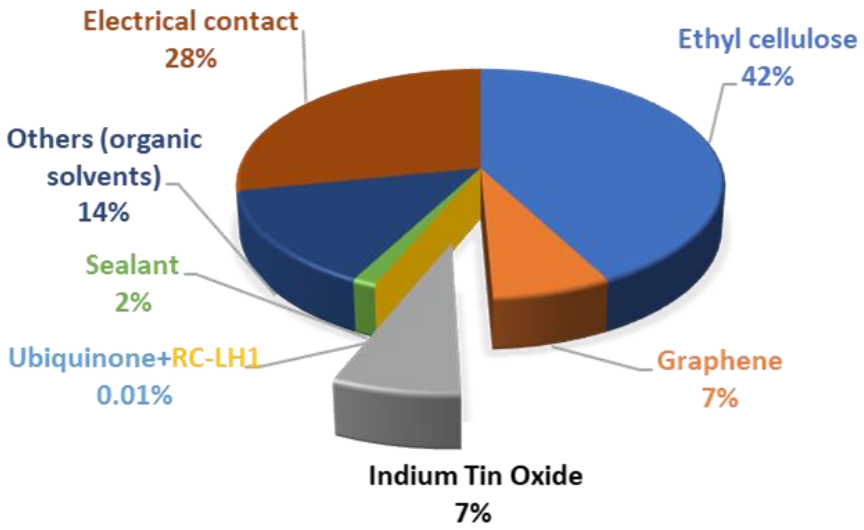

Supporting Figure S5. Usage break down of the ethyl-cellulose based photosynthetic protein solar cell per square centimetre of current produced: Estimate of the proportion of materials, by weight, used for cell fabrication. Both ITO and graphene can be recovered and reused.

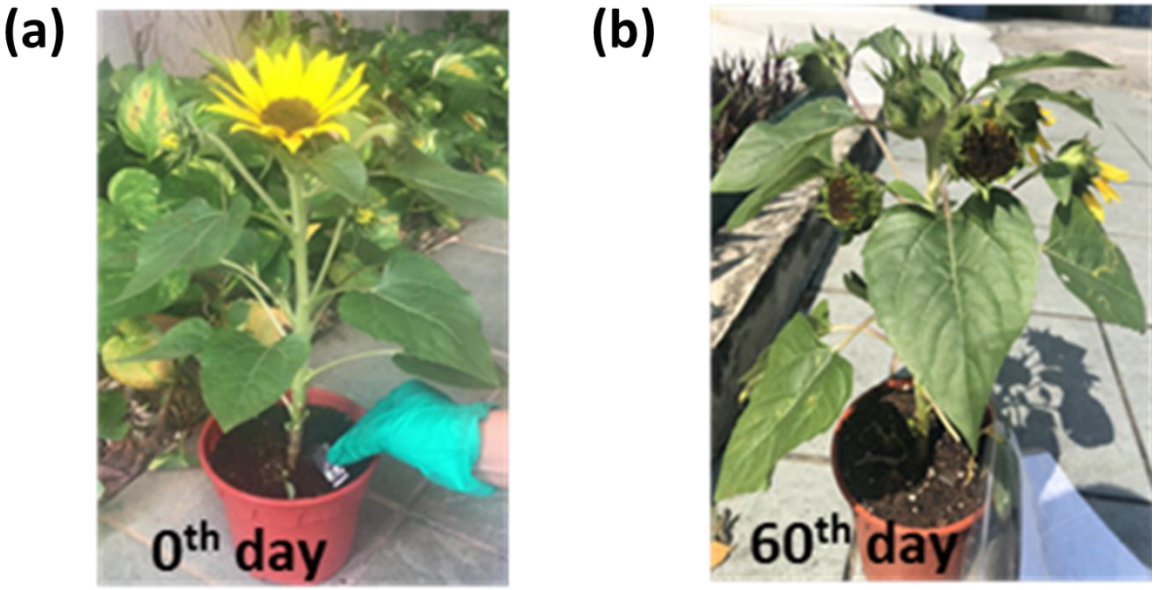

Supporting Figure S6. Biodegradation study: Discarded ten end of life devices buried in sunflower pot and watered regularly over 60 days. (a) zeroth day (b) sixtieth day of experiment.